cAMP receptor affinity controls wave dynamics, geometry and morphogenesis in *Dictyostelium*

Dirk Dormann[1], Ji-Yun Kim[2], Peter N. Devreotes[2] and Cornelis J. Weijer[1],*

[1]School of Life Sciences, Division of Cell and Developmental Biology, University of Dundee, Wellcome Trust Biocentre, Dow Street, Dundee, DD1 5EH, UK
[2]Department of Biological Chemistry, Johns Hopkins School of Medicine, Baltimore, MD 21205, USA
*Author for correspondence (e-mail: c.j.weijer@dundee.ac.uk)

SUMMARY

Serpentine G-protein-coupled cAMP receptors are key components in the detection and relay of the extracellular cAMP waves that control chemotactic cell movement during *Dictyostelium* development. During development the cells sequentially express four closely related cAMP receptors of decreasing affinity. In this study, we investigated the effect of cAMP receptor type and affinity on the dynamics of cell-cell signalling in vivo, by measuring the dynamics of wave initiation and propagation in a variety of cAMP receptor mutants. We found that receptor affinity controls the frequency of wave initiation, but it does not determine wave propagation velocity, thus resulting in dramatic changes in wave geometry. In the limiting case, the affinity of the receptor is so low that waves can still be initiated but no stable centres form - thus, the cells cannot aggregate. In mounds, expression of low affinity receptors results in slow concentric waves instead of the normally observed multi-armed spiral waves. Under these conditions there is no rotational cell movement and the hemispherical mounds cannot transform into slugs. These results highlight the importance of receptor number and affinity in the proper control of cell-cell signalling dynamics required for the successful completion of development.

Key words: cAMP receptor, Receptor affinity, cAMP relay, Wave propagation, Chemotaxis, Cell movement

INTRODUCTION

Development of multicellular organisms requires the spatio-temporal co-ordination of patterns of cell division, cell death, gene expression and cell movement, which involves cell-cell signalling via extracellular signals. These signals can be short or long range and can form spatial gradients (i.e. wingless during the patterning of the *Drosophila* imaginal discs (Strigini and Cohen, 2000; The and Perrimon, 2000)) or they can be relayed from cell to cell over large distances, as in the case of the propagating cAMP waves controlling chemotactic aggregation of starving cells of the social amoebae *Dictyostelium discoideum*. Whether signalling molecules form gradients or propagate as waves depends on the detailed kinetics of signal production, degradation and transport (Meinhardt, 1982). In vertebrates, proteins of the FGF, TGF-β and Wnt families are important signalling molecules that are detected via different receptor families. Each receptor family consists of several distinct members that differ in their ligand specificity and affinity (Boutros et al., 2000). Different affinity receptors for the same ligand may couple to different downstream signal transduction pathways. It has been proposed that high affinity receptors could turn on a response, whereas the low affinity receptors turn off the response at high concentrations of the ligand, resulting in a gaussian dose response curve, which may be important in the interpretation of the signals (Bray and Lay, 1994). In the case of signal relay it is to be expected that receptor number and affinity will determine the dynamics and therefore the information content (frequency, amplitude, duration and range) of the signal.

The social amoebae *Dictyostelium discoideum* provide a powerful system for studying the role of receptor subtypes (of different affinities) in controlling the dynamics of cell-cell signalling during multicellular development. The starvation-induced chemotactic aggregation of individual cells is controlled by propagating waves of the chemo-attractant cyclic AMP (Parent and Devreotes, 1996). The cAMP signals are periodically initiated by cells in aggregation centres and relayed by surrounding cells, to result in outward propagating waves of cAMP, which direct inward movement of the cells towards the aggregation centre. The cells detect the signal via specific cAMP receptors, activate the aggregation-specific adenylylcyclase (ACA) and produce and secrete additional cAMP. cAMP binding to the receptors also triggers an adaptation process, which results in a cessation of ACA activation and a shutdown of cAMP production. A highly specific secreted cAMP phosphodiesterase causes the extracellular cAMP levels to fall. When cAMP levels fall, the cells de-adapt and become responsive to new signals coming from the centre (Parent and Devreotes, 1999). Cells move up cAMP gradients as long as the signal is increasing over time (Wessels et al., 1996). cAMP not only controls cell movement during aggregation but is also a major regulator controlling the expression of developmentally regulated and cell-type specific genes (Firtel, 1996; Gerisch, 1987). cAMP waves also control the movement of the cells in all the later stages of development

Table 1. Properties of the different wildtype and mutant cAMP receptors used in this study*

Receptor type	Affinity K_d (nm)	EC$_{50}$ receptor phosphorylation (nm)	Receptors per cell	Developmental phenotype of receptor knock-out strains	Receptor number per cell×10^3	Development if expressed in cAR1^{null}/cAR3^{null} cells
cAR1	25±8‡ 230±45	30¶	~7×10^4** (4 hours starved)	No aggregation¶¶	75±38‡ 260±34	Fruiting bodies§§
cAR3	47±82‡ 680±280	NA	~5×10^3‡‡ (6 hours starved)	Fruiting bodies‡‡	16±24‡ 210±14	Large aggregation territories, normal fruiting bodies§§
N272	ND	1000¶	NA	NA	~300¶	No aggregation§§
IIIb21	7407±2628§	5000§	NA	NA	~300§	Inefficient aggregation§
cAR2	>5000‡	50,000¶	ND	Arrested at tight mound stage***	~400¶	No aggregation§§

*The receptors are ordered according to their affinity. The chimeric receptor N272 consists of the transmembrane domain of cAR1 and the cytoplasmic tail of the cAR2 receptor, as shown. The receptor IIIb21 is a cAR1 receptor with a single amino acid substitution (N229D) in the third extracellular loop. The K_d refers to the receptor affinity as measured in phosphate buffer. The EC$_{50}$ receptor phosphorylation represents the EC$_{50}$ of the cAMP-induced electrophoretic mobility shift of the receptors due to phosphorylation. The number of receptors per cell given is the number of cAMP binding sites per cell, for both wildtype cells that are starved for 4 hours (column 4) and vegetative cells overexpressing receptors under the constitutively active actin15 promoter (column 6). Columns 5 and 7 describe the developmental phenotype of the receptor gene knockout strains and cell lines overexpressing only one cAMP receptor in a cAR1^{null}/cAR3^{null} background respectively. ND, not determined; NA, not applicable.

‡Johnson et al., 1992; §Kim et al., 1997; ¶Kim and Devreotes, 1994; **Johnson et al., 1991; ‡‡Johnson et al., 1993; §§Kim et al., 1998; ¶¶Sun and Devreotes, 1991; ***Saxe et al., 1993.

(Dormann et al., 2000). The dynamics of the cAMP signals are essential for the proper control of cell movement and gene expression and therefore for development.

During aggregation the geometry and dynamics of the cAMP waves are accurately reflected by their associated darkfield waves, which are caused by cell shape changes in response to propagating cAMP waves (Alcantara and Monk, 1974; Tomchik and Devreotes, 1981). Darkfield waves can be observed in mounds as well, and we have shown recently that they reflect cAMP waves (Patel et al., 2000; Rietdorf et al., 1996; Siegert and Weijer, 1995).

During development the cAMP signal is detected and transduced by a family of at least four cAMP receptors (cAR1-cAR4), which differ in their expression levels and patterns. The cAMP receptor types expressed sequentially during development have decreasing affinities for cAMP (Table 1), possibly to enable the organism to cope with an increase in extracellular cAMP concentrations during the formation of the multicellular structures (Abe and Yanagisawa, 1983; Kim et al., 1998). The high affinity receptor cAR1 is the first to be expressed during early aggregation, it is the primary receptor responsible for aggregation since cells lacking cAR1 fail to aggregate (Sun and Devreotes, 1991; Sun et al., 1990). cAR1 has two distinct affinity states of ~30 and ~300 nM under physiological conditions (Johnson et al., 1992). These different affinity states most likely reflect covalent modifications (e.g. phosphorylation) and/or the interaction with intracellular effectors (e.g. G proteins). cAR1 continues to be expressed in later development in all cells. During later aggregation a small number of cAR3 receptors are expressed. Deletion of cAR3

has no obvious phenotype (i.e. cAR3 null cells are still able to complete development and form fruiting bodies (Johnson et al., 1993)). In the slug, the expression of cAR3 becomes confined to the prespore cells (Yu and Saxe, 1996). cAR2 is first expressed at the mound stage where it is restricted to cells in the forming prestalk zone. The affinity of cAR2 is low and can hardly be measured by a standard cAMP binding assay. However, the measurement of the cAMP-dependent phosphorylation of the receptor's cytoplasmic tail shows an EC$_{50}$ of ~50 μM, at least 1000-fold higher than the EC$_{50}$ of cAR1 (Kim et al., 1998). Deletion of cAR2 arrests development at the mound stage (Saxe et al., 1993). At the slug stage the low affinity receptor cAR4 is expressed in a prestalk-specific manner. Deletion of cAR4 leads to defects during culmination (Louis et al., 1994).

Using mutants that express only one receptor type under the control of a strong constitutive promoter it has been shown that cAR1, cAR3 and cAR2 can couple to the cAMP relay and chemotaxis signal transduction pathways in aggregation stage cells in vitro when stimulated with saturating doses of cAMP (Kim et al., 1998). However, this does not tell us what roles these receptors play in the dynamics of the cAMP signalling and chemotaxis in vivo. Here the cells have to respond to signals that they produce themselves, giving rise to complex interactions between signal amplitude, frequency and receptor affinity. Furthermore, at any given stage during development there is likely to be more than one cAMP receptor expressed (most likely on the same cells). Therefore the contribution of each receptor type to the signalling events remains to be determined.

To dissect the influence of different receptors we have investigated the dynamics of darkfield wave initiation and propagation in mutants that overexpress either cAR1, affinity mutants of cAR1, cAR2, cAR3 or the cAR1/cAR2 chimera N272 in a cAR1/cAR3 double null background (RI9), which in itself is completely unresponsive to stimulation with cAMP. The cAMP sensitivity of the investigated receptors can be put in the following order: cAR1 (highest affinity)>cAR3>N272> IIIb21>cAR2 (lowest affinity) (Table 1). We have carefully quantified the optical density wave frequencies and propagation speeds and found that lower affinity receptors result in lower frequencies of wave initiation. Surprisingly, once initiated, wave speed was not strongly dependent on receptor affinity. In the mound stage the dependence of wave frequency on receptor affinity persisted, although it was less pronounced than during aggregation.

MATERIALS AND METHODS

Strains, culture and development

All *Dictyostelium* strains were grown axenically in HL-5 medium at 22°C (Sussman, 1987), the transformed strains had an additional 20 µg/ml G418 (Sigma). The medium for the uracil auxotroph parental strain DH1 was supplemented with 0.2 mM uracil (Amresco). The mutant cell lines used were the same as those generated and characterised previously (Kim et al., 1997; Kim et al., 1998; Johnson et al., 1993; Saxe et al., 1993). The genes for the different cAMP receptors and the mutant receptors IIIb21 and N272 were expressed ectopically in a cAR1^{null}/cAR3^{null}-cell line under the control of the actin15 promoter. Cells were harvested in the exponential growth phase (2-6×10^6 cells/ml), washed once in KK2 phosphate buffer (20 mM KH$_2$PO$_4$/K$_2$HPO$_4$, pH 6.8) and plated on KK2 agar (1% Difco Bacto-Agar in KK2) at a density of 8×10^5 cells/cm^2. The plates were incubated in the dark at 22°C.

Videomicroscopy

Optical density waves during the early stages of aggregation were monitored using darkfield optics (Gross et al., 1976). A single plano-convex lens with a diameter of 10 cm (f=15 cm) was used, similar to a previous set-up (Siegert and Weijer, 1989). A CCD camera (JAI 1020) with a zoom objective (Cosmicar TV Zoom 12.5-75 mm) and a 2× magnification lens was used to acquire the images.

The signal waves in aggregation streams and mounds were observed on an Axiovert 25 microscope (Zeiss, objectives: CP-Achromat 10×/NA 0.25 Ph1 Var1, Plan-Neofluar 2.5×/NA 0.0075). The annular stop slider at the condenser was arrested in the middle position between brightfield and phase-contrast (Ph1) to create the oblique illumination that is essential for the detection of optical density waves in these stages (Siegert and Weijer, 1995). A JAI 2040 camera was attached to the camera port via a 0.5× video adapter (Zeiss).

The video signals were digitised with an IC-PCI-board (AM-CLR acquisition module, Imaging Technology Inc.). The control of the image capturing board, the recording of time-lapse sequences and the subsequent analysis were performed with the Optimas software (Optimas Corporation, Version 5.2).

Analysis of image sequences

Time-space plots were generated to measure velocity and period of optical density waves during both early aggregation and mound stage (Siegert and Weijer, 1989; Siegert and Weijer, 1995). Basically, the grey values along a fixed line were stored for all the images of a sequence. The position of this line was such that waves travelled perpendicular to it. Afterwards these lines were displayed beneath each other in their temporal order, thus generating a time axis in Y-direction. The wave velocity could be derived from the slope of the resulting wave bands, and the period derived by measuring the distance between consecutive waves in Y-direction.

A new method was developed to determine the velocity of dark-field waves in the mutants where waves were initiated only once at random positions. We basically calculated the distance that the wave travelled over a period of time by using image multiplication to superimpose two images taken some time apart (Russ, 1995). If the time interval between these images was chosen appropriately, distinct wave fronts appeared and the distance covered during this time interval could be measured to give an estimate of the speed of wave propagation. Image subtraction of pairs of successive images was routinely used to enhance the visibility of optical density waves especially in the mound stage to determine the exact wave geometry's (Siegert and Weijer, 1995). This method detects the differences between images, the propagating waves, while unchanged structures and background are effectively suppressed.

RESULTS

Wave propagation during early aggregation

One of the first signs of aggregation is the appearance of darkfield waves a few hours after the onset of starvation. Analysis and quantitation of these waves in the different wild-type strains and cAMP-receptor expressing cell lines revealed remarkable differences in the wave patterns they produced. These results are summarised in Fig. 1. The original parent strain for all cell lines, Ax3, was used as a reference. Wave propagation and cell movement have been investigated in detail both during aggregation and the mound stage of development (Rietdorf et al., 1996). Previously, we have shown that Ax3 forms predominantly spiral waves (Fig. 1A). The parent for the receptor mutants, DH1, is a uracil auxotroph that was produced from Ax3 by a deletion of the *pyr5-6* gene coding for the Uridin-monophosphate-synthase (Caterina et al., 1994). In contrast to Ax3, DH1 showed predominantly concentric waves in this set of experiments (Fig. 1B). To analyse the temporal behaviour at different positions in space we constructed time space plots (Fig. 1G) (Siegert and Weijer, 1989; Siegert et al., 1994). The waves were initiated periodically by aggregation centres (Fig. 1G). The three bright vertical lines indicate the positions of centres that appear brighter due to the accumulation of cells. Around 20 waves were emitted by each centre. The slanted lines, emanating from the centres, represent individual outward propagating wave fronts. The slope of these lines is a measure of wave velocity. Upon collision the waves annihilate and will form the boundaries of the aggregation territories (dark vertical lines).

The cAR1/RI9 cell line, which only expresses the highest affinity cAR1 receptor, is able to develop to fruiting bodies. During early aggregation it also produced concentric optical density waves like its parent DH1 (Fig. 1C). However, the waves arose in different random positions and no clear centres were established. Only few centres could be found that fired repeatedly. This difference with DH1 is clear in the time-space-plots of DH1 and cAR1/RI9 (Fig. 1G,H). The waves in DH1 originate in one line, whereas the signals in cAR1/RI9 do not arise from one line in the time space plots. The waves appear less frequent in cAR1/RI9 than in either Ax3 or DH1. The similar slopes of the lines in the time space plots (Fig. 1G,H)
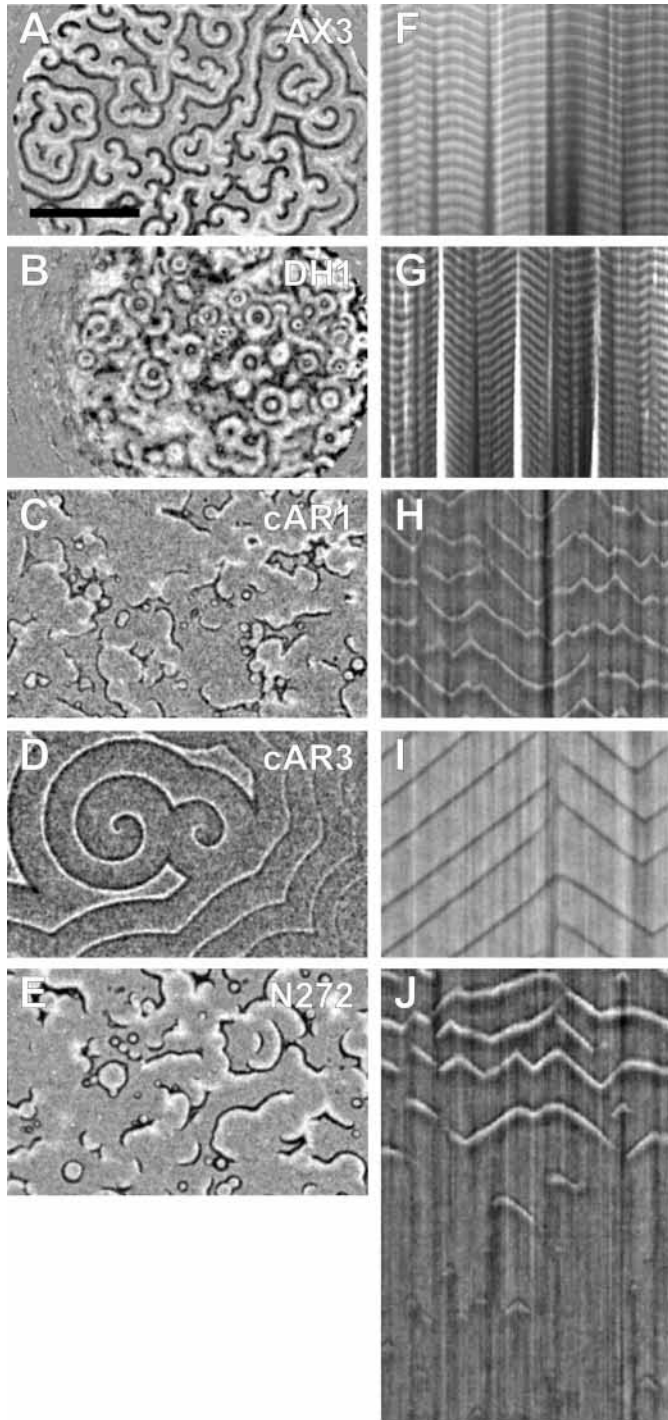
Fig. 1. Comparison of the darkfield wave patterns during early aggregation. The left column A-E shows the actual wave patterns of the different wild-type and mutant strains at the same scale (Bar, 10 mm). All images were enhanced by image subtraction. The according time-space plots are displayed in the right column, F-J. They all cover a period of 67 minutes (200 images), except for N272 (J) with 133 minutes (400 images) to show the disappearance of the waves. The vertical axis of the time-space plots corresponds to the time axis, time increases from the top to the bottom. (A,F) Wild-type strain Ax3 with spiral waves. (B,G) Parental strain DH1 with concentric waves. (C,H) cAR1 mutant with concentric waves. (D,I) cAR3 mutant with spiral waves. (E,J) N272 mutant with concentric waves.

indicate that waves propagate at comparable speeds. These chaotic optical density waves in cAR1/RI9 disappear during aggregation and are replaced by fixed oscillating centres (Fig. 2A-D), which oscillate at high frequency (Fig. 2E,F). These fast oscillating centres will organise small aggregation territories, which go on to develop into mounds and slugs.

The car3/RI9 mutant, which expresses the slightly lower affinity receptor car3, showed a completely different wave pattern, characterised by large wave fronts that are often organised into large spirals (Fig. 1D). These spirals covered territories much larger than those seen in the Ax3 strain (Fig. 1A). The time-space plots showed that the frequency of spiral rotation was slow, but that the wave propagation speed was not much different from the wildtype (Fig. 1I). Cells of this strain went on to aggregate, to form mounds and finally fruiting bodies.

We next investigated N272/RI9, this line expresses a chimeric cAR1/cAR2 receptor with an EC_{50} of around 1 μM cAMP (Table 1; Kim et al., 1998). This strain produced concentric waves, which again originated at different random positions (Fig. 1E). The centres fired only once from a given position as can be seen in the time-space plot (Fig. 1J). Since the cells did not generate signals coming from a fixed centre, they randomly moved up wave fronts coming from different directions and, as a result, could not aggregate. This behaviour is similar to that shown by the car1/RI9 cells during early development. However, in N272/RI9, fixed centres never appeared. Instead, the darkfield waves disappeared completely after 10.6±1.0 hours (n=6). The time-space-plot shows that this was a sudden process, which affected all the cells on the plate simultaneously (Fig. 1J), indicative of a precisely timed process. It seems most likely that the actin15 promoter loses its activity during later development and that the number of N272 receptors decreases below a critical level, insufficient to sustain further wave propagation. Further development was nearly arrested at this stage. In some cases a few aggregation centres per plate emerged after a delay of several hours. Most dispersed again after a number of hours but some persisted and managed to form tiny fruiting bodies.

The cAR2/RI9 mutant, overexpressing the low affinity receptor cAR2 didn't show any signs of darkfield waves at all and was unable to aggregate (data not shown). These cells were not sensitive enough to detect the small changes in the extracellular cAMP that normally initiate aggregation. Attempts to stimulate these cells with cAMP to induce mound formation failed. We conducted chemotaxis assays with a cAMP-filled glass micropipette placed in a field of aggregation-competent cells. At high cAMP concentrations (10^{-2}-10^{-1} M cAMP) the cells were attracted by the electrode, as can be seen by the pile of cells that has accumulated around the tip of the glass electrode (Fig. 3A). At concentrations that elicit a positive response in DH1 or cAR1/RI9 (10^{-4} M cAMP), the cAR2/RI9 cells show no reaction towards the electrode (Fig. 3B). Synergy experiments of 5% fluorescence-labelled cAR2/RI9 cells with 95% unlabelled DH1 cells showed that a small number of cAR2/RI9 cells managed to co-aggregate with DH1, whereas labelled RI9 cells, which are completely unresponsive to cAMP, did not co-aggregate (data not shown). This clearly shows that the cAR2/RI9 cells can respond to signals secreted by the parent strain DH1, most likely cAMP, albeit not very efficiently.
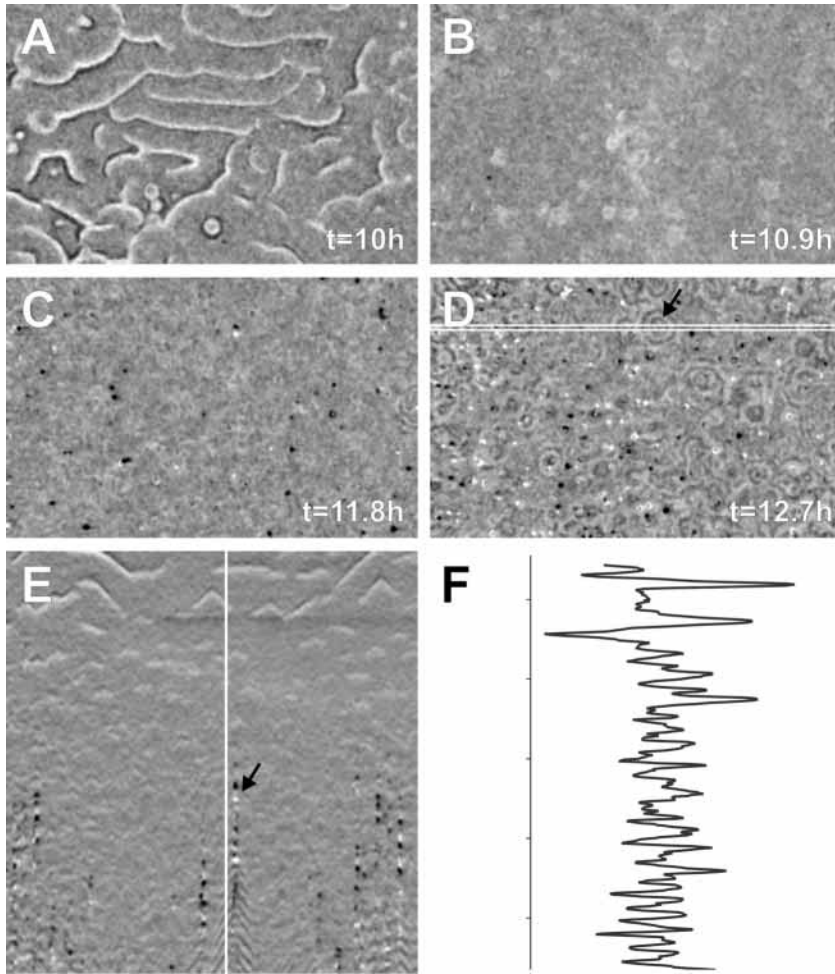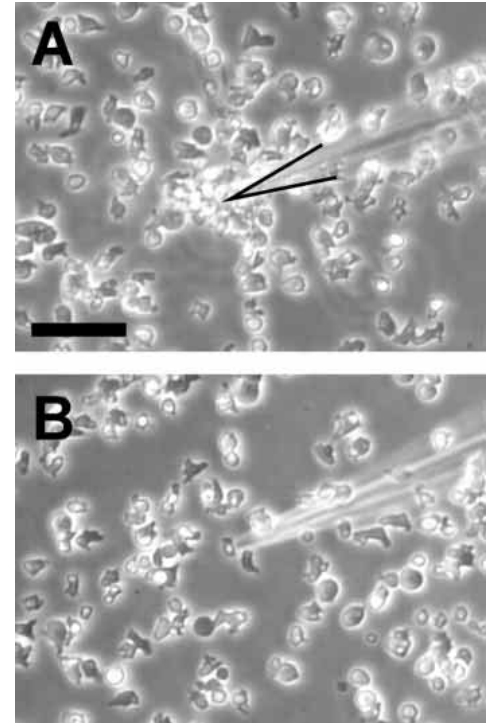
Fig. 2. Change from long period random waves to short period waves emitted by centres in cAR1/RI9. (A-D) Images of darkfield waves at successive stages of development. (E) Time-space plot of the experiment shown in (A-D) measured along the horizontal white line in D. (F) Change of optical density over time, read out along the white line shown in D. The black arrows in D,E indicate the position of a centre

Fig. 3. Chemotactic response of cAR2/RI9 cells. (A) Positive response of aggregation-competent cells, 38 minutes after the cAMP-filled electrode (10^{-1} M cAMP) had been introduced. The cells have moved chemotactically towards the tip of the electrode and piled up. The outline of the tip in the cell mass is indicated in black. (B) The cAMP concentration in the electrode was 10^{-4} M, too low to be detected by the cAR2/RI9 cells. The cells remain evenly spread. The photograph was taken after about 38 minutes as well. Bar, 50 μm.

## cAMP-receptor affinity affects wave geometry in the mound stage

Waves of cAMP can be observed as optical density waves in the mound stage. In mounds of the wild-type strain Ax3, we found mostly multi-armed spiral waves, which confirmed previous observations (Rietdorf et al., 1996; Siegert and Weijer, 1995). DH1, which during aggregation produced concentric waves, was organised in the mound by multi-armed spiral waves. An example of a nine-armed spiral wave is shown in Fig. 4A. In Fig. 4E the wave fronts are shown as bold curved lines with arrows indicating counter clockwise rotational movement around the central core region. As during aggregation, the cells move towards the signal source leading to counter rotational cell movement. Often, mounds of DH1 transformed into rings that also showed many propagating waves. Rings could contract to reform mounds or break up and move away to fuse with other rings (Dormann et al., 1998). In both cases, regular shaped mounds formed again and development continued.

Mounds of the cAR1/RI9 strain showed preferentially single armed spiral waves (Fig. 4B) that rotated around a core located at the centre of the mound. Ring formation was observed in some cases (Fig. 4J), the number of wave fronts was lower than in ring-shaped DH1 mounds (data not shown). The cAR3/RI9 mounds often exhibited a complex wave pattern that appeared to be a mixture of concentric and spiral waves. These spiral waves did not rotate around the centre of the mound. Their cores were positioned in different parts of the mound, resulting in an unusual wave system somewhere in between concentric and spiral waves (Fig. 4G). In N272/RI9, as mentioned earlier, mound formation was a rare event. However, in some cases mounds appeared 13 hours after the initiation of development. We found concentric waves in all cases ($n=6$). Fig. 4D shows a snapshot of such an event, where the bright ring-shaped wave has almost reached the border of the mound. In three cases the waves disappeared during the recording, accompanied by a flattening and expansion of the whole mound. There were no waves in another three mounds. It appears that even if a mound is formed, the pacemaker generating the waves is unstable. After 24 hours, fruiting bodies had formed in the parental strain
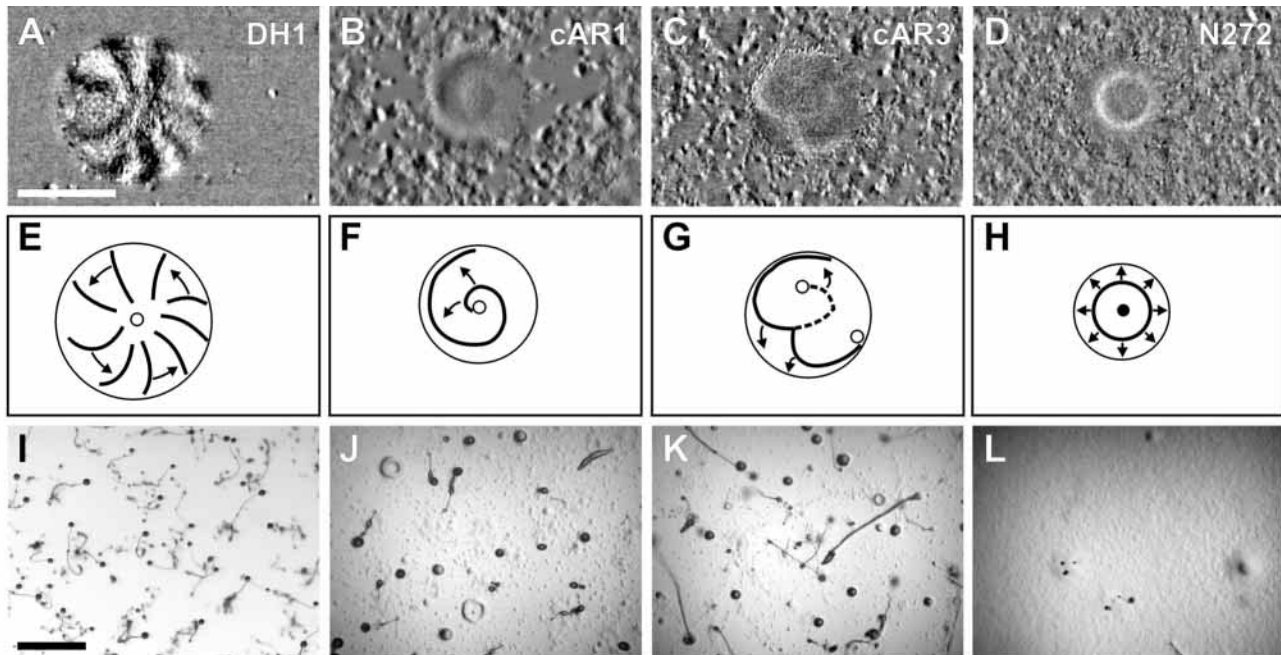
Fig. 4. Optical density waves in mounds. Subtracted images of the mounds (A-D) reveal the wave pattern. Due to the image processing the wave fronts appear as black and white bands. Bar, 250 μm. In the schematic representations in the middle row (E-H), waves are shown as bold black lines and the direction of wave propagation is indicated by little arrows. Small circles represent the cores around which the spiral waves rotate, whereas the black dot in H marks the position from which concentric waves originated periodically. The outline of the mounds is indicated by a thin black line. The final phenotype after 24 hours is shown in the bottom row (I-L). (A,E,I) Parental strain DH1 with multi-armed spiral waves. (B,F,J) cAR1 mutant with single-armed spiral wave. (C,G,K) cAR3 mutant with complex wave patterns. (D,H,L) N272 mutant with concentric waves.

DH1 (Fig. 4I). In the cAR1/RI9 and cAR3/RI9 mutants a considerable number of mounds and rings were still present at this time (Fig. 4J,K), but these strains seemed to undergo normal development. However, the N272 strain failed to aggregate efficiently. In some cases, tiny fruiting bodies developed from a few of the mounds that appeared (Fig. 4L).

We had previously suggested that the formation of multi-armed spirals could be due to the expression of the low affinity receptor cAR2 at the mound stage (Vasiev, 1997). To test this possibility we examined darkfield wave propagation in mounds of cAR2 null mutants. The development of these cells is arrested or severely delayed at the mound stage (Saxe et al., 1993). In mounds of cAR2 null strains there were clear multi-armed spirals (Fig. 5A,C). The other receptor, whose expression starts at the early mound stage is cAR3. There were multi-armed spirals in the cAR3null strain as well (Fig. 5B,D). These observations clearly show that the sudden appearance of multi-armed spiral waves is not linked to the expression of either cAR2 or cAR3, as originally proposed. However, multi-armed spirals were less frequent in the cAR1/RI9 and cAR3/RI9 strains, suggesting that high levels of expression of a high affinity receptor can suppress multi-armed spiral formation. Since the number of cAR1 receptors decreases in wild-type cells after aggregation, this decrease in high affinity receptors could be responsible for lowering the excitability and the appearance of multi-armed spiral waves.

The period of DH1 darkfield waves could easily be determined from the time-space plots, because the waves were generated by oscillating centres that remained at spatially fixed positions (Fig. 1G). In some of the cell lines, waves were initiated only once and at random positions. To obtain comparable periodicity data for these mutants we measured time intervals between waves passing through a fixed point in a plate, irrespective of their origin, reflecting the excitability of the system. This was carried out for three different positions in each time-space-plot. Typical data are shown for all the cell lines in Fig. 6 and all the data are summarised in a histogram in Fig. 7. The lines expressing variant receptors showed a three- to fourfold longer period compared with the parental strain
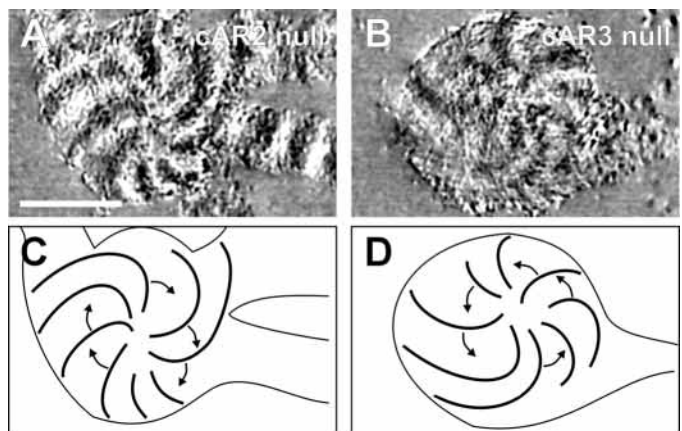
Fig. 5. Multi-armed spirals in the cAR2 and cAR3 null strains. (A) Multi-armed spirals in a mound of the cAR2[null] strain. (B) Multi-armed spiral in a mound of the cAR3 [null] strain. (C,D) Schematic diagrams of the waves visible in A,B and an indication of their direction of propagation. Bar, 250 μm.

Fig. 6. Frequency of darkfield waves measures in DH1, cAR1/RI9, cAR3/RI9 and N272/RI9 in at the aggregation and mound stage. Typical traces of the oscillations measured at one point in an aggregation field (left column) and in mounds (right column).


DH1 (Fig. 7A). The variation in period length was also much higher for the mutant lines. DH1 darkfield waves had the shortest period of 3.5±0.3 minutes, followed by cAR3 (9.9±4.6 minutes) and then by the slow waves in cAR1 (11.6±4.0 minutes). N272, expressing the receptor with the lowest affinity that still produced waves, showed the longest period (14.3±4.3 minutes). cAR1 centres represent the period of oscillating cAR1 centres that emerged after the randomly appearing waves had vanished (5.1±0.6 minutes). Although they are faster than the slow irregular waves that arise initially, the frequency of these waves coming from fixed centres is still significantly lower than those of DH1.

The same trend was observed at the mound stage (Fig. 7B). DH1 exhibited the shortest period. The mutants show longer periods as the parent strain DH1, with N272 showing the longest periods. However, the differences between the strains in the mound stage seem to be much smaller than during early aggregation. These data indicate that receptor sensitivity has an effect on the periodicity, such that lower affinity results in longer periods caused by less frequent initiation of waves.

cAMP receptor affinity does not determine wave propagation speed

We measured wave propagation speed and period during the aggregation stage and in mounds. The velocity of the darkfield waves seemed to be quite constant over time in the three mutants cAR1, cAR3 and N272 and even their average velocities were similar (cAR1 204±33 µm/minute; cAR3 231±39 µm/minute; N272 215±34 µm/minute). Thus wave propagation velocity is not determined by receptor affinity. Fig. 8A shows the distribution of the wave velocities. The data were grouped into classes with a width of 25 µm/minute and

Fig. 7. Frequency distribution of the period of optical density waves in early aggregation and in the mound stage. The data were divided into classes with a width of 40 seconds and normalised to account for the different number of measurements. (A) Period of darkfield waves during early aggregation. DH1 shows the shortest period, whereas all the other mutants are shifted towards the longer periods. (B) Period of waves in the mound stage. The periods are generally shorter in the mound stage, however the mutants still have longer periods.
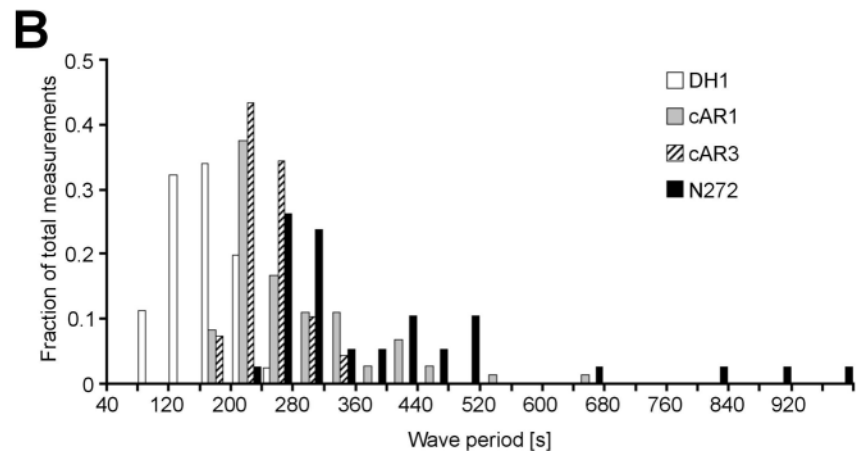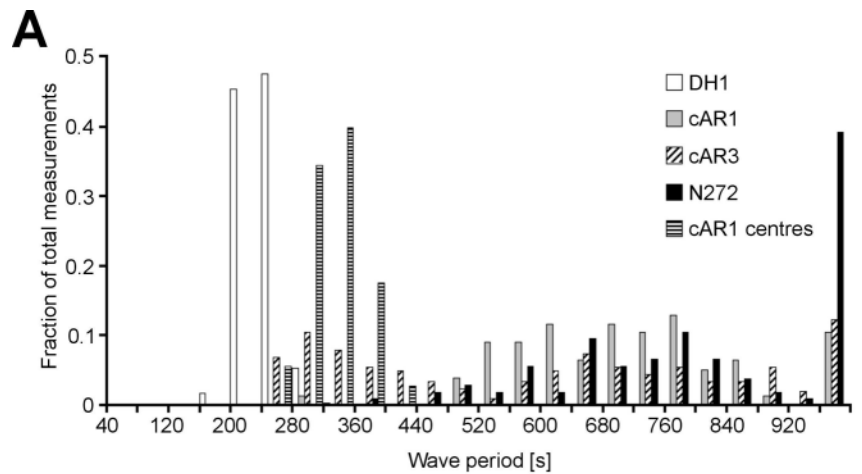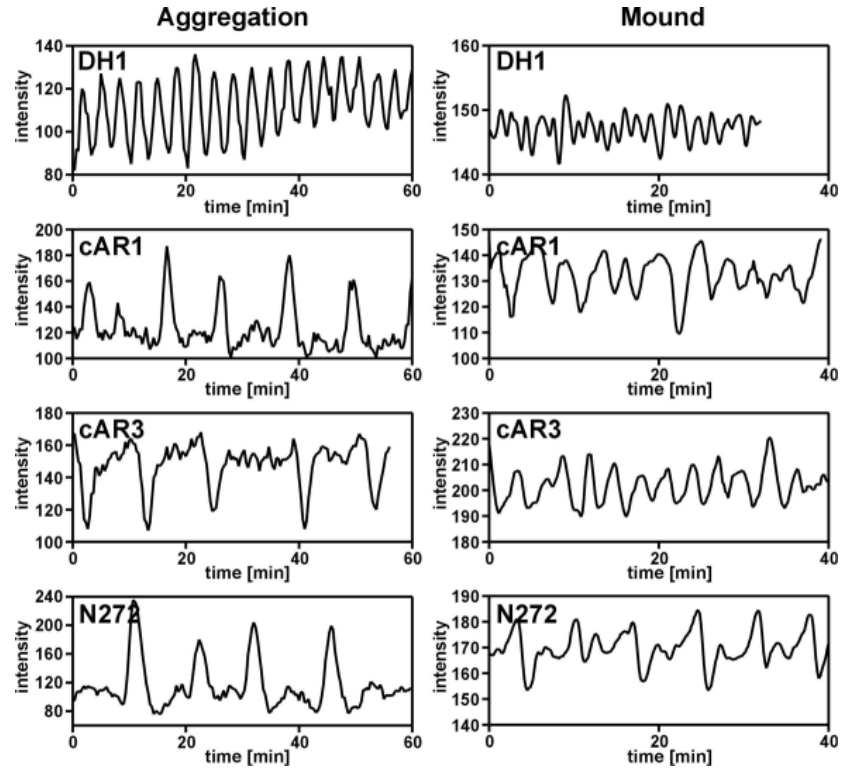
normalised to account for the different numbers of measurements per mutant. The values for the mutants peaked in the two classes ranging from 200 to 250 µm/minute. The parental strain DH1 showed a much broader distribution instead and the peak was shifted towards the higher values. This reflects the fact that the velocity of DH1 darkfield waves changed during the course of development. It decreased from maximum values of more than 500 µm/minute to around 150 µm/minute, resembling the Ax2 and Ax3 strains, where this process has been well documented (Rietdorf et al., 1996; Siegert and Weijer, 1989).

In mounds, wave propagation velocity was roughly the same in all four strains (Fig. 8B). In comparison to the darkfield waves in early aggregation (Fig. 8A), wave velocity in mounds was reduced to 16-25% (40-55 µm/minute). We did not investigate in detail whether this decrease was a continuous process. In DH1 mounds with aggregation streams, wave speed was already reduced to 60.2±9.1 µm/minute (n=10) and declined further to 51.2±8.1 µm/minute (n=16) in older mounds without aggregation streams. This suggests that the main velocity changes took place at a slightly earlier stage, possibly coinciding with the formation of cell-cell contacts and streams.

The receptor subtypes have different affinities for cAMP, but there are also structural differences between them, which may affect their function. To further investigate the relationship between wave initiation frequency and affinity, we studied mutants that express receptors in which the affinity for cAMP had been changed by single amino acid substitutions. We investigated mutants IIb21, IIb22 and IIIb22 (Kim et al., 1997) and found that only IIIb21 produced darkfield waves (Fig. 9A). This receptor has been shown to have an affinity of around 10 µM, slightly higher than N272 (Table 1). This mutant initiated random waves and never fired from the same centre twice. Although the wave propagation speed is only marginally slower than that from the mutant N272, the average local wave period was at least double (Fig. 9C,D). The waves eventually disappeared, as in the case of N272 (Fig. 9B). Sometimes small cell accumulations formed that looked like early mounds, although we have never observed any OD waves in these structures. This strain never develops into fruiting bodies under our conditions. These results clearly show that the differences in wave parameters are primarily linked to the affinity of the cAMP receptor and not to small structural differences between the receptors.

Fig. 8. Frequency distribution of wave velocities during early aggregation and in the mound stage. The data were divided into classes with a width of 25 µm/minute and normalised to account for the different number of measurements. (A) Distribution of the velocities of darkfield waves. The mutants show a similar distribution, whereas the parental strain DH1 is slightly shifted towards higher values. (B) Distribution of the velocities of optical density waves in the mound stage. The velocities of the four strains are essentially the same.

DISCUSSION

Wave initiation frequency depends on receptor affinity

To date, it has proven to be difficult to assign unique roles in cAMP signalling to the different cARs expressed during development because they are all able to couple to cAMP relay, chemotaxis and gene-expression under in vitro conditions using saturating cAMP signals (Table 1; Kim et al., 1998; VerkerkeVanWijk et al., 1998). Our results show that during early aggregation wave initiation frequency is strongly dependent on receptor affinity, a decrease in affinity of the cAR receptors results in a decrease of wave initiation frequency (Fig. 7). This can be understood in the following way. In cells expressing only low affinity cAMP receptors it takes longer to build up the local cAMP concentration to a level where it can stimulate a sufficient number of low affinity receptors to elicit a cAMP relay response. This will result in a time lag before autocatalytic cAMP production gets going. However, once auto-catalysis has started, the local cAMP concentrations will build up rapidly until adaptation prevents further cAMP production (Devreotes and Steck, 1979; Klein et al., 1985). Neighbouring cells will be stimulated with levels of cAMP sufficiently high to initiate autocatalytic cAMP production immediately, resulting in waves propagating at normal speed.
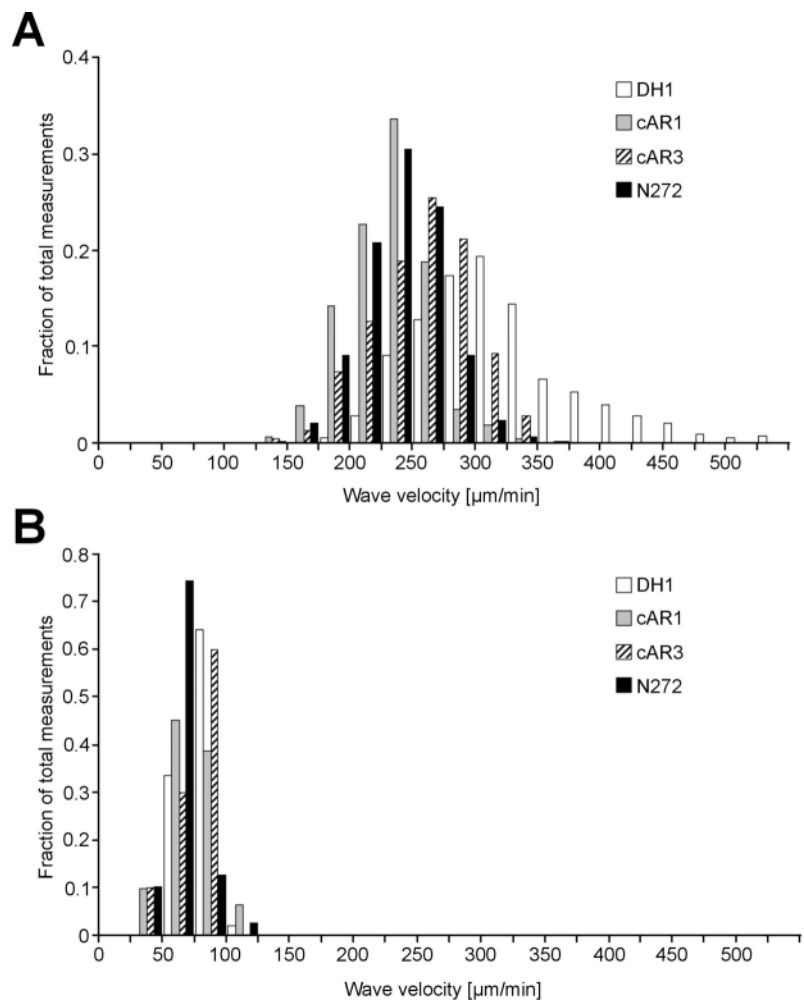
Fig. 9. The frequency of wave initiation in the cAR1 affinity receptor mutants. Histogram showing the distribution of wave initiation periods and wave velocities of the mutant IIIb21 at the aggregation stage of development. The waves are concentric and the mutants do not fire successive wave from the same centre. Consequently, the cells do not aggregate. (A) Concentric darkfield wave initiated in random locations. (B) Time-space plot showing the disappearance of the waves after 6 hours. (C,D) Comparison of wave velocity and period between IIIb21 and N272.
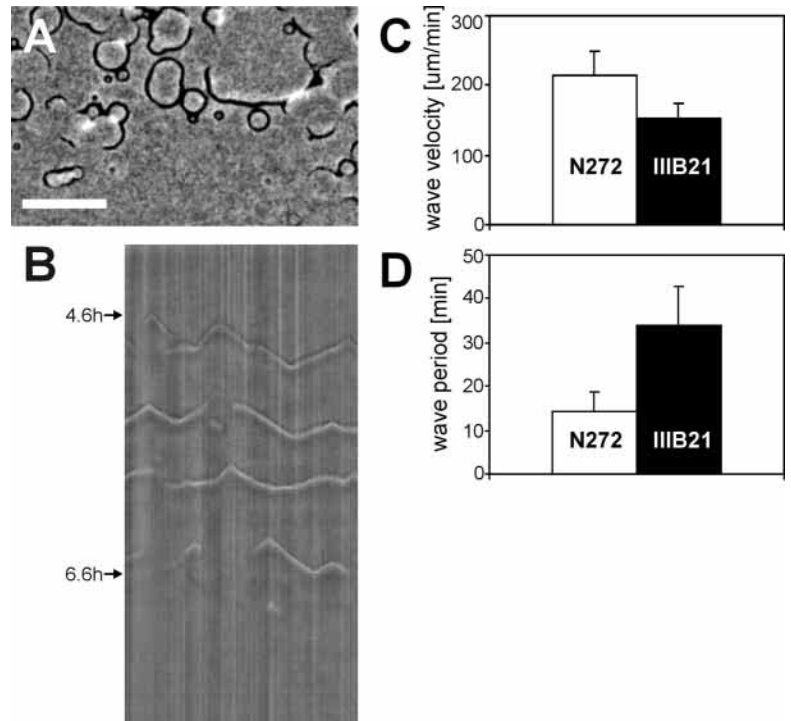
The decrease in frequency at normal wave propagation speed results in a longer wavelength of the cAMP signal as can be seen clearly in the large spiral waves observed during aggregation of cAR3/RI9.

Remarkably, none of the mutants investigated could initiate waves with the same frequency as the parent strains Ax3 and DH1. Since cAR1 is the major receptor expressed during aggregation, one would expect that expression of the cAR1 receptor in the RI9 mutant would result in a phenotype which resembled that of the parent strain DH1. This is not the case, DH1 emits periodically concentric darkfield waves from aggregation centres at fixed locations (Fig. 1B,G), whereas cAR1/RI9 initiates waves at lower frequency in completely random locations during early aggregation, typical of the behaviour observed in the strains expressing the low affinity receptors. Expression under the control of the actin15 promoter results in at least fivefold overexpression of cAR1 during early aggregation, as determined by cAMP-binding studies (Table 1; Johnson et al., 1991). The observed reduction in wave initiation frequency suggests that overexpression of cAR1 could have a partial dominant negative effect on cAMP relay in vivo. This effect is not observed in vitro under saturating assay conditions where the cells are able to give normal amplitude responses (Kim et al., 1998). It therefore seems likely that the great number of receptors sequester limiting amounts of cAMP, without being able to transduce the signal efficiently to activate adenylylcyclase. Possibly not all receptors are coupled to intracellular signal transduction components such as G proteins during the early stages of aggregation, where these components may be limiting.

The cAR3/RI9 strain could set up stable aggregation centres emitting large spiral waves, which organised in large aggregation territories in agreement with earlier observations (Kim et al., 1998). From theoretical considerations it is known that spirals can persist in excitable media, whereas concentric waves need at least pacemaker cells in the centre (Durston, 1973). Since we never observed concentric waves during aggregation in cAR3/RI9, we consider it most likely that these cells are only excitable, in contrast to wild-type cells, which are in an oscillatory mode during aggregation. Although biochemical experiments have shown that the affinities of the cAR1 and cAR3 receptors are only slightly different, these in vivo experiments show that differences in receptor structure may lead to physiological significant changes in signal transduction efficiency not previously detected in biochemical experiments.

Influence of cAR affinity on centre formation

Our results show that there exists a close correlation between the frequency of wave initiation and the formation of stable aggregation centres. All the mutants that show a low frequency of wave initiation also have difficulty in forming stable signalling centres (Fig. 1E; Fig. 9B). During development, cells go from being non-excitable by cAMP at the vegetative stage, to being excitable during early aggregation, to being able to produce cAMP in an oscillatory manner (Gerisch, 1982; Lax, 1979). This evolution of the signalling system reflects the pulse-controlled increase in expression of essential components of the signalling system such as cAMP receptors, Gα2, cAMP phosphodiesterase and the aggregation-stage-specific adenylylcyclase (ACA) (Aubry and Firtel, 1999; Parent and Devreotes, 1996). Not all cells go through this developmental pathway at the same pace, resulting in considerable heterogeneity in the individual cell's make-up of signal transduction components (Weeks and Weijer, 1994; Weijer et al., 1984a; Weijer et al., 1984b). Aggregation centres therefore most likely arise in random positions, where, by chance, a number of cells have come into close vicinity that secrete enough cAMP and are sensitive enough to cAMP to trigger autocatalytic cAMP production and initiate a cAMP wave. As the wave propagates outward, surrounding cells move towards the source of the signal, thus resulting in accumulation of cells at the site of wave initiation. Since more cells can produce more cAMP faster, this increases the probability to initiate a second cAMP wave from the same centre. The mutant strains that express the low affinity receptors take longer before they can raise the extracellular cAMP to levels where it comes into the regime of autocatalysis again. During this time the cells start to disperse again owing to their continuous random movement. This dispersal then results in a destabilisation of the centre and a new centre will be formed by chance somewhere else. Thus, centre stabilisation may require a fine

balance between the period of the cAMP signals and its resulting chemotactic accumulation of cells in the centre and dispersal of the cells in the centre due to random movement.

The regulation of wave propagation speed during development

During normal development, wave velocity decreases from 800 μm/minute to ~250 μm/minute (Rietdorf et al., 1996; Siegert and Weijer, 1989). This change in wave propagation speed was not observed in any of the cAR mutant strains, which always propagate waves at ~250 μm/minute (Fig. 8A). During the early development of wild-type strains the first receptor to be expressed is cAR1. Initially, the number of cAR1 receptors is low but then their numbers rapidly increase since their expression is under the feedback control of the cAMP pulses. During this time the wave propagation speed decreases rapidly. The cAR mutants investigated in this study express cAR receptors at already higher numbers from the beginning of development (Table 1) and don't show this decrease in speed. This would suggest that high receptor numbers somehow result in lower wave propagation speed by an as yet unknown mechanism. In mounds, the wave propagation speed is low (60 μm/minute, Fig. 8B). The cells are now in tight contact and the extracellular space between the cells is small. We think it likely that the densities of cAR receptors and extracellular phosphodiesterase become so high that the cAMP produced by a given cell is only able to stimulate its immediate neighbours. Under these conditions wave propagation speed is set by the delay between a cell detecting cAMP at its front end and being able produce and secrete enough cAMP to stimulate the cell immediately behind it. This delay therefore should be less then 10 seconds to result in the wave propagation speeds observed.

REFERENCES

Abe, K. and Yanagisawa, K. (1983). A new class of rapid developing mutants in *Dictyostelium discoideum*: implications for cyclic AMP metabolism and cell differentiation. *Dev. Biol.* **95**, 200-210.

Alcantara, F. and Monk, M. (1974). Signal propagation during aggregation in the slime mould *Dictyostelium discoideum*. *J. Gen. Microbiol.* **85**, 321-334.

Aubry, l. and Firtel, R. (1999). Integration of signalling networks that regulate *Dictyostelium* differentiation. *Annu. Rev. Cell. Dev. Biol.* **15**, 469-517.

Boutros, M., Mihaly, J., Bouwmeester, T. and Mlodzik, M. (2000). Signalling specificity by frizzled receptors in *Drosophila*. *Science* **288**, 1825-1828.

Bray, D. and Lay, S. (1994). Computer-simulated evolution of a network of cell-signaling molecules. *Biophys. J.* **94**, 972-977.

Caterina, M. J., Milne, J. L. S. and Devreotes, P. N. (1994). Mutation of the third intracellular loop of the cAMP receptor, cAR1, of Dictyostelium yields mutants impaired in multiple signaling pathways. *J. Biol. Chem.* **269**, 1523-1532.

Devreotes, P. N. and Steck, T. L. (1979). cAMP relay in *Dictyostelium discoideum*. II. Requirements for the initiation and termination of the response. *J. Cell Biol.* **80**, 300-309.

Dormann, D., Vasiev, B. and Weijer, C. J. (1998). Propagating waves control *Dictyostelium discoideum* morphogenesis. *Biophys. Chem.* **72**, 21-35.

Dormann, D., Vasiev, B. and Weijer, C. J. (2000). The control of chemotactic cell movement during *Dictyostelium* morphogenesis. *Philos. Tran. R. Soc. Lond. B Biol. Sci.* **355**, 983-991.

Durston, A. J. (1973). *Dictyostelium discoideum* aggregation fields as excitable media. *J. Theor. Biol.* **42**, 483-504.

Firtel, R. A. (1996). Interacting signaling pathways controlling multicellular development in *Dictyostelium*. *Curr. Opin. Genet. Dev.* **6**, 545-554.

Gerisch, G. (1982). Dynamics of cyclic AMP signal generation and cell-development in *Dictyostelium discoideum*. *Hoppe-Seyler's Z. Physiol. Chemie.* **363**, 535-536.

Gerisch, G. (1987). Cyclic AMP and other signals controlling cell development and differentiation in *Dictyostelium*. *Annu. Rev. Biochem.* **56**, 853-879.

Gross, J. D., Peacey, M. J. and Trevan, D. J. (1976). Signal emission and signal propagation during early aggregation in Dictyostelium discoideum. *J. Cell Sci.* **22**, 645-656.

Johnson, R. L., Vaughan, R. A., Caterina, M. J., Van Haastert, P. J. M. and Devreotes, P. N. (1991). Overexpression of the cAMP receptor-1 in growing *Dictyostelium* cells. *Biochemistry* **30**, 6982-6986.

Johnson, R. L., Van Haastert, P. J. M., Kimmel, A. R., Saxe, C. L., III, Jastorff, B. and Devreotes, P. N. (1992). The cyclic nucleotide specificity of three cAMP receptors in *Dictyostelium*. *J. Biol. Chem.* **267**, 4600-4607.

Johnson, R. L., Saxe, C. L., III, Gollop, R., Kimmel, A. R. and Devreotes, P. N. (1993). Identification and targeted gene disruption of cAR3, a cAMP receptor subtype expressed during multicellular stages of *Dictyostelium* development. *Genes Dev.* **7**, 273-282.

Kim, J. Y. and Devreotes, P. N. (1994). Random chimeragenesis of G-protein-coupled receptors - Mapping the affinity of the cAMP chemoattractant receptors in *Dictyostelium*. *J. Biol. Chem.* **269**, 28724-28731.

Kim, J. Y., Caterina, M. J., Milne, J. L. S., Lin, K. C., Borleis, J. A. and Devreotes, P. N. (1997). Random mutagenesis of the cAMP chemoattractant receptor, cAR1, of *Dictyostelium* - mutant classes that cause discrete shifts in agonist affinity and lock the receptor in a novel activational intermediate. *J. Biol. Chem.* **272**, 2060-2068.

Kim, J. Y., Borleis, J. A. and Devreotes, P. N. (1998). Switching of chemoattractant receptors programs development and morphogenesis in *Dictyostelium*: receptor subtypes activate common responses at different agonist concentrations. *Dev. Biol.* **197**, 117-128.

Klein, C., Fontana, D., Knox, B., Theibert, A. and Devreotes, P. (1985). cAMP receptors controlling cell-cell interactions in the development of *Dictyostelium*. *Cold Spring Harb. Symp. Quant. Biol.* **50**, 787-799.

Lax, A. J. (1979). The evolution of excitable behaviour in *Dictyostelium*. *J. Cell Sci.* **36**, 311-321.

Louis, J. M., Ginsburg, G. T. and Kimmel, A. R. (1994). The cAMP receptor CAR4 regulates axial patterning and cellular differentiation during late development of *Dictyostelium*. *Genes Dev.* **8**, 2086-2096.

Meinhardt, H. (1982). Models of biological pattern formation. London: Acad. Press.

Parent, C. A. and Devreotes, P. N. (1996). Molecular genetics of signal transduction in *Dictyostelium*. *Annu. Rev. Biochem.* **65**, 411-440.

Parent, C. A. and Devreotes, P. N. (1999). A cell's sense of direction. *Science* **284**, 765-770.

Patel, H., Guo, K. D., Parent, C., Gross, J., Devreotes, P. N. and Weijer, C. J. (2000). A temperature-sensitive adenylyl cyclase mutant of *Dictyostelium*. *EMBO J.* **19**, 2247-2256.

Rietdorf, J., Siegert, F. and Weijer, C. J. (1996). Analysis of Optical-Density Wave-Propagation and Cell-Movement During Mound Formation in *Dictyostelium-Discoideum*. *Dev. Biol.* **177**, 427-438.

Russ, J. (1995). The Image Processing handbook. Boca Raton, Ann Arbor, London, Tokyo: CRC Press.

Saxe, C. L., III, Ginsburg, G. T., Louis, J. M., Johnson, R., Devreotes, P. N. and Kimmel, A. R. (1993). CAR2, a prestalk cAMP receptor required for normal tip formation and late development of *Dictyostelium discoideum*. *Genes Dev.* **7**, 262-272.

Siegert, F. and Weijer, C. (1989). Digital image processing of optical density wave propagation in *Dictyostelium discoideum* and analysis of the effects of caffeine and ammonia. *J. Cell Sci.* **93**, 325-335.

Siegert, F. and Weijer, C. J. (1995). Spiral and concentric waves organize multicellular *Dictyostelium* mounds. *Curr. Biol.* **5**, 937-943.

Siegert, F., Weijer, C. J., Nomura, A. and Miike, H. (1994). A gradient method for the quantitative analysis of cell movement and tissue flow and its application to the analysis of multicellular *Dictyostelium* development. *J. Cell Sci.* **107**, 97-104.

Strigini, M. and Cohen, S. M. (2000). Wingless gradient formation in the *Drosophila* wing. *Curr. Biol.* **10**, 293-300.

Sun, T. J. and Devreotes, P. N. (1991). Gene targeting of the aggregation stage cAMP receptor cAR1 in *Dictyostelium*. *Genes Dev.* **5**, 572-582.

Sun, T. J., Van Haastert, P. J. M. and Devreotes, P. N. (1990). Surface cAMP receptors mediate multiple responses during development in *Dictyostelium* - evidenced by antisense mutagenesis. *J. Cell Biol.* **110**, 1549-1554.

Sussman, M. (1987). Cultivation and synchronous morphogenesis of *Dictyostelium* under controlled experimental conditions. *Methods Cell Biol.* **28**, 9-29.

The, I. and Perrimon, N. (2000). Morphogen diffusion: the case of the wingless protein. *Nat. Cell Biol.* **2**, 79-82.

Tomchik, K. J. and Devreotes, P. N. (1981). Adenosine 3′,5′-monophosphate waves in *Dictyostelium discoideum*: a demonstration by isotope dilution-fluorography technique. *Science* **212**, 443-446.

Vasiev, B. N., Siegert F., Weijer C. J. (1997). Multiarmed spirals in excitable media. *Phys. Rev Lett.* **78**, 2489-2492.

VerkerkeVanWijk, I., Kim, J. Y., Brandt, R., Devreotes, P. N. and Schaap, P. (1998). Functional promiscuity of gene regulation by serpentine receptors in *Dictyostelium discoideum*. *Mol. Cell. Biol.* **18**, 5744-5749.

Weeks, G. and Weijer, C. J. (1994). The *Dictyostelium* cell cycle and its relationship to differentiation. *FEMS Microbiol. Lett.* **124**, 123-130.

Weijer, C. J., McDonald, S. A. and Durston, A. J. (1984a). A frequency difference in optical-density oscillations of early *Dictyostelium discoideum* density classes and its implications for development. *Differentiation* **28**, 9-12.

Weijer, C. J., McDonald, S. A. and Durston, A. J. (1984b). Separation of *Dictyostelium discoideum* cells in density classes throughout their development and their relation to the later cell types. *Differentiation* **28**, 13-23.

Wessels, D., Shutt, D., Voss, E. and Soll, D. R. (1996). Chemotactic decisions by *Dictyostelium* amoebae in spatial gradients and natural waves of cAMP are made by pseudopods formed primarily off the substratum. *Mol. Biol. Cell* **7**, 1349-1349.

Yu, Y. M. and Saxe, C. L. (1996). Differential distribution of cAMP receptors cAR2 and cAR3 during *Dictyostelium* development. *Dev. Biol.* **173**, 353-356.